Mott-insulator-to-superconductor transition in a two-dimensional superlattice

Rubem Mondaini,[1] Predrag Nikolić,[2] and Marcos Rigol[1]

[1] *Department of Physics, The Pennsylvania State University, University Park, PA 16802, USA*
[2] *School of Physics, Astronomy and Computational Sciences, George Mason University, Fairfax, VA 22030, USA and Institute for Quantum Matter at Johns Hopkins University, Baltimore, MD 21218, USA*

We use quantum Monte Carlo and exact diagonalization calculations to study the Mott-insulator to superconductor quantum phase transition in a two-dimensional fermionic Hubbard model with attractive interactions in the presence of a superlattice potential. The model introduced offers unique possibilities to study such transitions in optical lattice experiments. We show that, in regimes with moderate to strong interactions, the transition belongs to the $3D$-XY universality class. We also explore the character of the lowest energy charge excitations in the insulating and superconducting phases and show that they can be fermionic or bosonic depending on the parameters chosen.

PACS numbers: 71.10.Fd, 02.70.Uu

arXiv:1412.1829v3 [cond-mat.str-el] 6 Oct 2015

INTRODUCTION

The traditional microscopic approach to understanding superconductivity scrutinizes the pairing instability of a "parent" normal state [1]. If this normal state is not a conventional state of weakly interacting electrons (i.e., a Fermi liquid or a band-insulator), then the emerging superconductivity is not ordinary either. Many superconductors fall in this category, including organic, heavy-fermion, and all high-temperature ones (cuprates and iron-based). Non-trivial electron correlations behind superconductivity are most famously seen in the "pseudogap" state of cuprates, and are very difficult to understand from experimental observations [2–9]. This is where ultracold-atom systems, which are highly tunable, are expected to help. However, the temperatures required to realize the d-wave pairing of cuprates remain prohibitively low for current ultracold atom experiments [10]. Even obtaining long-range antiferromagnetic correlations in a three-dimensional Mott insulator remains a challenge [11–13].

With these challenges in mind, it is desirable to design s-wave paired states that would make the "pseudogap" physics accessible to current experiments with ultracold fermions. Here, we study a zero temperature Mott insulator of bound Cooper pairs, which gives rise to the s-wave analogue of a pseudogap state, as well as to a superconductor upon changing lattice parameters. We consider a Fermi-Hubbard model in the square lattice in the presence of a superlattice potential, with Hamiltonian

$$\hat{H} = -t \sum_{\langle \boldsymbol{i}\,\boldsymbol{j}\rangle,\sigma} (\hat{c}^\dagger_{\boldsymbol{i}\sigma}\hat{c}_{\boldsymbol{j}\sigma} + \text{H.c.}) - t' \sum_{\langle\langle \boldsymbol{i}\,\boldsymbol{j}\rangle\rangle,\sigma} (\hat{c}^\dagger_{\boldsymbol{i}\sigma}\hat{c}_{\boldsymbol{j}\sigma} + \text{H.c.})$$
$$+U \sum_{\boldsymbol{i}} \left(\hat{n}_{\boldsymbol{i}\uparrow} - \frac{1}{2}\right)\left(\hat{n}_{\boldsymbol{i}\downarrow} - \frac{1}{2}\right) + \Delta \sum_{\boldsymbol{i},\sigma} (-1)^{(i_x+i_y)} \hat{n}_{\boldsymbol{i}\sigma}, \quad (1)$$

where $c^\dagger_{\boldsymbol{i}\sigma}$ ($c_{\boldsymbol{i}\sigma}$) are the fermionic creation (annihilation) operators at site $\boldsymbol{i}$, with (pseudo-)spin $\sigma =\uparrow,\downarrow$, and $\hat{n}_{\boldsymbol{i}\sigma} = \hat{c}^\dagger_{\boldsymbol{i}\sigma}\hat{c}_{\boldsymbol{i}\sigma}$ are the corresponding site occupation operators. The nearest and next-nearest hopping amplitudes are denoted by t and t' [$\langle \boldsymbol{i}\,\boldsymbol{j}\rangle$ and $\langle\langle \boldsymbol{i}\,\boldsymbol{j}\rangle\rangle$ indicate sums over nearest and next-nearest neighbor sites $\boldsymbol{i}$ and $\boldsymbol{j}$], respectively, the strength of the on-site attractive interaction by $U < 0$, and of the staggered potential by Δ.

In experiments, attractive interactions between atoms can be generated using Feshbach resonances [14], optical superlattices can be created using arrays of laser beams [15–17], and periodically modulated optical lattices allow to control the relative amplitudes and phases between nearest and next-nearest neighbor hopping parameters [18, 19]. A recent experimental realization of the Haldane model exemplifies these capabilities [20]. We stress as a caveat to be kept in mind that, in experiments using Feshbach resonances, the single-band description based on Eq. (1) fails when the gap between different Hubbard bands is not much larger than the other energy scales involved in the problem [21–23].

To show what makes the model in Eq. (1) special to study Mott-insulator to superconductor phase transitions, we analyze it in two limits. In the non-interacting limit ($U = 0$), $\hat{H}$ can be diagonalized in $\mathbf{k}$-space, which unveils two bands, $E(\mathbf{k}) = -4t' \cos k_x \cos k_y \pm \sqrt{\epsilon^2_{\mathbf{k}} + \Delta^2}$, where the reduced Brillouin zone is given by $|k_x + k_y| \leq \pi$ and $|k_x - k_y| \leq \pi$, and $\epsilon_{\mathbf{k}} = -2t\,[\cos(k_x) + \cos(k_y)]$ is the dispersion relation in the presence only of nearest neighbors hopping. For $t' < t/\sqrt{2}$, an indirect gap opens for $\Delta_c = 2t'$ [between $(\pm\pi,0)$ in the lower band and $(\pm\pi/2, \pm\pi/2)$ in the upper band]. For $t' > t/\sqrt{2}$, an indirect gap opens for $\Delta_c = 4t' - t^2/t'$ [between $(\pm\pi,0)$ in the lower band and $(0,0)$ in the upper band]. Δ_c is the critical value of Δ for the formation of a band insulator at half filling, i.e., a finite value of t' stabilizes a metallic state for nonzero values of Δ.

The other important limit is the one in which $U/t \neq 0$ but $t' = 0$. Recalling that the attractive Hubbard Hamiltonian can be mapped onto a repulsive one by the down-spin particle-hole transformation [24], $\hat{c}_{\boldsymbol{i}\downarrow} \leftrightarrow (-1)^{i_x+i_y}\,\hat{c}^\dagger_{\boldsymbol{i}\downarrow}$, the staggered potential transforms

as $\Delta\sum_{i\sigma}(-1)^{(i_x+i_y)}\hat{n}_{i\sigma} \rightarrow h\sum_{i}(-1)^{(i_x+i_y)}\hat{S}^z_i$, with $\hat{S}^z_i = (\hat{n}_{i\uparrow} - \hat{n}_{i\downarrow})/2$ and $h = 2\Delta$. Therefore, at half-filling, the staggered potential in the attractive model is equivalent to a staggered z-magnetic field in the repulsive one. For $h = 0$, the ground state of the repulsive Hubbard model is an $SU(2)$ symmetric Mott insulator that exhibits long-range antiferromagnetic correlations. Those translate onto long-range s-wave superconducting order and charge density-wave order in the attractive model (i.e., a supersolid) [24]. An infinitesimal h breaks $SU(2)$ symmetry and the ground state of the repulsive model becomes an S^z antiferromagnet, which translates onto a (charge density-wave) Mott insulator in the attractive case, i.e., superconductivity is destroyed for any nonzero value of Δ. For large values of h, this insulator can be understood to be the result of pinning the pairs to the sites with energies $-\Delta$, which precludes transport.

Now if one takes the $U = 0$ limit with $t' \neq 0$ and $\Delta < \Delta_c$ as the starting point, adding weak attractive interactions generates superconductivity, i.e., contrary to the $t' = 0$ case, superconductivity is possible for $\Delta \neq 0$. Increasing Δ, one can then destroy the superconductor in favor of a Mott-insulator. Such a transition is the focus of this work. It can be driven in real time in ultracold fermion experiments by tuning lattice parameters. This is to be contrasted to the Mott-insulator to superconductor transition in the cuprates, which requires changing doping, i.e., the filling would need to be changed in real time to drive such a transition in optical lattices.

We study Hamiltonian (1) in $L\times L$ lattices using two unbiased computational approaches: zero-temperature (projector) determinantal quantum Monte Carlo (PDQMC) [25, 26] and Lanczos exact diagonalization (ED). We focus on half-filled systems ($n = \langle n_{i\uparrow}\rangle + \langle n_{i\downarrow}\rangle = 1.0$, $\langle n_{i\uparrow}\rangle = \langle n_{i\downarrow}\rangle$), except when analyzing the nature of the charge excitations. The projector parameter in the PDQMC calculations was set to $\Theta t = 40$, ensuring that the we obtain ground state properties for lattices with up to 256 sites, while the imaginary time discretization step was taken to be $\delta\tau = 0.1$. In the ED calculations, we used translational symmetries, which allowed us to solve lattices with up to 16 sites. $t = 1$ sets the energy scale in all results reported in what follows.

RESULTS

Figure 1 depicts the phase diagram for Eq. (1), obtained using ED [Fig. 1(a)] and PDQMC [Fig. 1(b)], as given by the Δ_c necessary to drive the superconductor to Mott-insulator transition as a function of $|U|$ and t'. Important features visible in Fig. 1 are, (i) Δ_c decreases with increasing $|U|$, and, (ii) as expected from the discussion in the noninteracting limit, Δ_c increases with increasing t'. The first trend can be understood as both the attractive interaction and the staggered potential favor

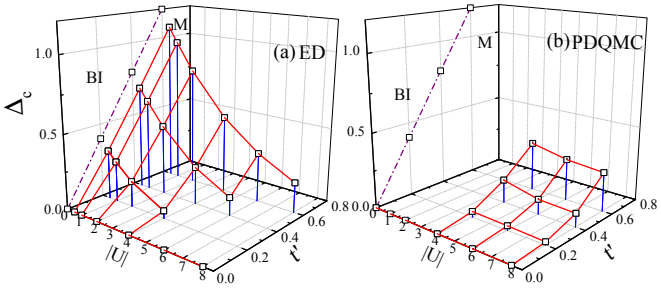

FIG. 1. (Color online) Phase diagram of Eq. (1) obtained via ED (a) and PDQMC (b). For $U/t = 0$, the dashed line marks the boundary between the metallic and band-insulating phases obtained analytically. For nonzero U, the surface formed by connecting the points (which report Δ_c) delimits the insulating ($\Delta > \Delta_c$) and superconducting ($\Delta < \Delta_c$) phases. Comparing (a) and (b), one can see that Δ_c is overestimated in the ED calculations due to finite-size effects.

local pair formation and, consequently, reduce long-range order when $\Delta \neq 0$ and $|U|$ is increased. The second trend follows from the fact that the delocalization promoted by t' competes with the pinning induced by Δ and U, and enhances superconductivity.

In the ED calculations, in order to determine Δ_c for the superconductor to Mott-insulator transition at fixed U and t', we use the ground-state fidelity metric [27–33]

$$\mathrm{g}(\Delta) = \frac{2}{L^2}\frac{1 - |\langle\Psi_0(\Delta)|\Psi_0(\Delta+\delta\Delta)\rangle|}{(\delta\Delta)^2}, \qquad (2)$$

where $|\Psi_0(\Delta)\rangle$ is the ground-state wavefunction of the Hamiltonian for a given staggered on-site energy Δ and $\delta\Delta$ is chosen to be small enough that the results for $\mathrm{g}(\Delta)$ are independent of its value. $\mathrm{g}(\Delta)$ is expected to exhibit a diverging (with increasing system size) maximum as one crosses a second order phase transition [27–33].

Figures 2(a)–2(c) depict the fidelity metric for different values of the onsite interaction ($U = -2$, -4 and -6, respectively) and for four values of t' ($t' = 0.0$, 0.2, 0.4 and 0.6). For $t' = 0$ and all values of U, one can see that there is a single peak in g for $\Delta \simeq 0$. This peak signals the supersolid to Mott-insulator transition previously discussed for the limit $U \neq 0$ but $t' = 0$. The signature of such a transition can still be seen for $t' \neq 0$ in the form of a peak at $\Delta \simeq 0$ with a height that decreases with increasing t' (notice the log scale in the y-axes). A second peak then emerges for $t' \neq 0$ signaling the superconductor to Mott-insulator transition with increasing Δ. We take the position of the maximum of this peak as the value of Δ_c predicted by ED. The compilation of these peak positions provides the phase diagram reported in Fig. 1(a). Notice that, with increasing $|U|$, the positions of the peaks for a given value of t' move towards smaller values of Δ. They also become broader and at some point merge with the one at $\Delta \simeq 0$. At that point, we cannot determine Δ_c using ED. This is why the phase diagram in Fig. 1(a) is

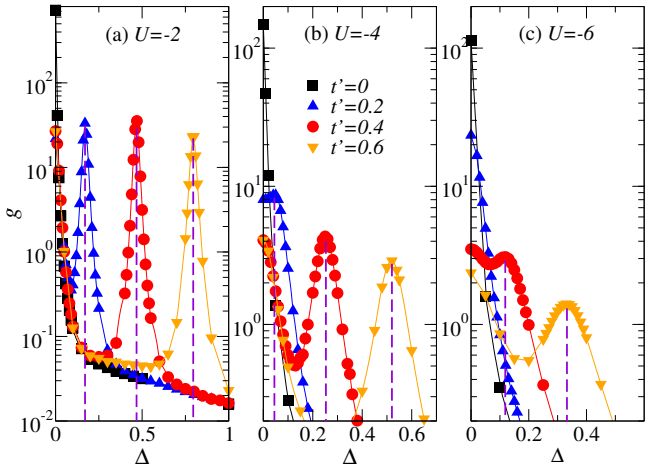

FIG. 2. (Color online) ED results for the fidelity metric vs Δ in 4×4 lattices at half-filling, for fours values of t' ($t' = 0$, 0.2, 0.4 and 0.6), and three values of U [$U = -2$ (a), -4 (b) and -6 (c)]. For $t' = 0$, the only peak seen in g is the one associated with the destruction of superconductivity for any nonzero value of Δ, whereas for finite values of t' a second peak appears at finite values of Δ signaling the superconductor to Mott-insulator transition.

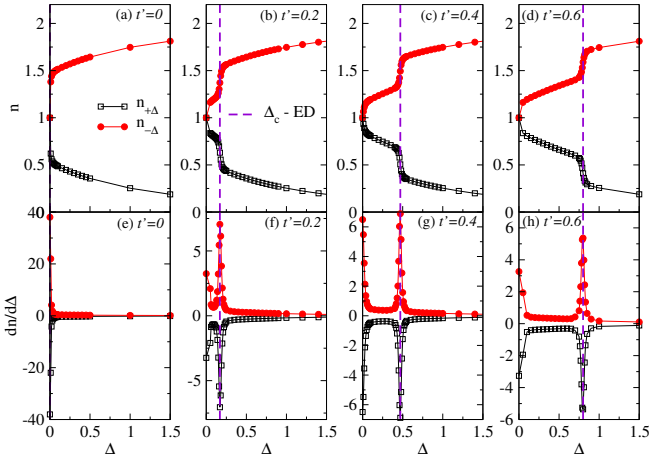

FIG. 3. (Color online) (a)–(d) Site occupation $\langle \hat{n}_{i\uparrow} + \hat{n}_{i\downarrow} \rangle$ in each sublattice (labeled by $n_{+\Delta}$ and $n_{-\Delta}$) as a function of Δ for different values of t' and $U = -2$. Vertical dashed lines mark the superconductor-insulator transition obtained through the fidelity metric. (e)–(h) Derivative of the site occupations in (a)–(d) with respect to Δ. All results were obtained by means of ED in a 4×4 lattice at half-filling.

missing points for large $|U|$ and small t' values.

Other quantities also show clear signatures of the transition. In the presence of the superlattice potential, the sublattices forming the bipartite square lattice possess different onsite energies and, consequently, the site occupation is different in the two site species. Figures 3(a)–3(d) display the site occupation in each sublattice as a function of Δ for $U = -2$ and several values of t'. As expected, as Δ increases, the difference between the site occupation in the sublattices increases. Remarkably, there is a sharp increase in this difference that occurs exactly at the value of Δ for which the fidelity metric predicts the superconductor to Mott-insulator transition. This sharp increase leads to a sharp peak in the derivative of the site occupation with respect to Δ, see Figs. 3(e)–3(h), which resembles the peak seen in the fidelity metric.

Another observable that exhibits clear signatures of the superconductor to Mott-insulator transition is the binding energy

$$E_b = 2E_0(n+1) - E_0(n+2) - E_0(n), \qquad (3)$$

where $E_0(n)$ correspond to the ground state energy of a system with n fermions.

Figure 4 shows the binding energy vs Δ for different values of U and t'. The trend is similar in all of them: for small values of Δ, before the superconductor to Mott-insulator transition for nonzero t' takes place, the energy associated with the pairs decreases, and then a dip occurs exactly at the transition point as detected by the fidelity metric. For larger values of Δ, in the Mott insulating phase, the binding energy steadily increases with increasing Δ.

In turn, similar robustness against the selection of the observable used to characterize the transition is seen in the PDQMC calculations of much larger lattice sizes than those amenable to exact diagonalization. An observable of much interest in experiments with ultracold fermions in optical lattices is the double occupancy. It was used, e.g., in Ref. [34] to detect the Mott insulating phase when increasing the onsite repulsion between fermions. In Fig. 5, we plot the double occupancy in the two sublattices vs Δ for $U = -4$ and different values of t' in a

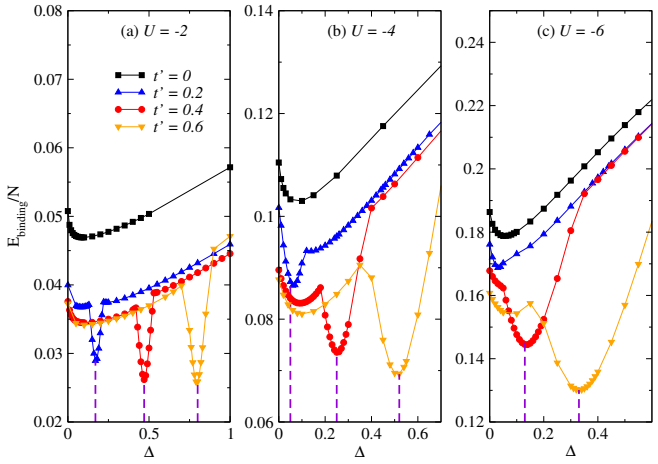

FIG. 4. (Color online) Binding energy as a function of Δ for $U = -2, -4$ and -6, and different values of t'. The dashed lines, which coincide with the minimum in the dips of the binding energy, report the values of Δ_c provided by the fidelity metric. All results were obtained by means of ED in a 4×4 lattice at half-filling.

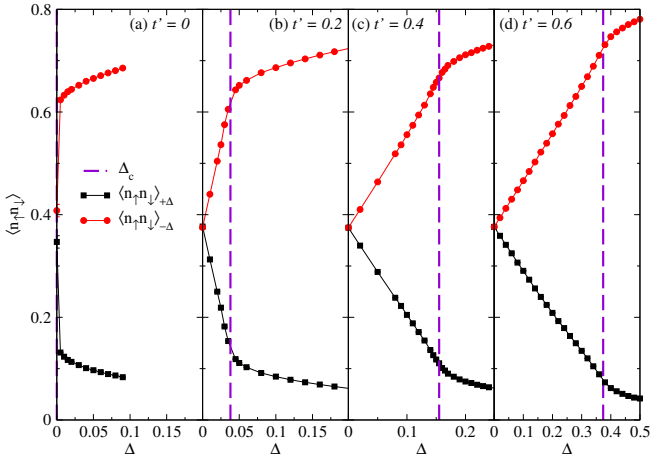

FIG. 5. (Color online) Double occupancy in the two sublattices as a function of Δ for $U = -4$ and different values of t'. These results were obtained using PDQMC in a 14×14 lattice at half filling. The vertical dashed lines depict the value of Δ_c as obtained in the finite-size scaling analysis of the pair structure factor.

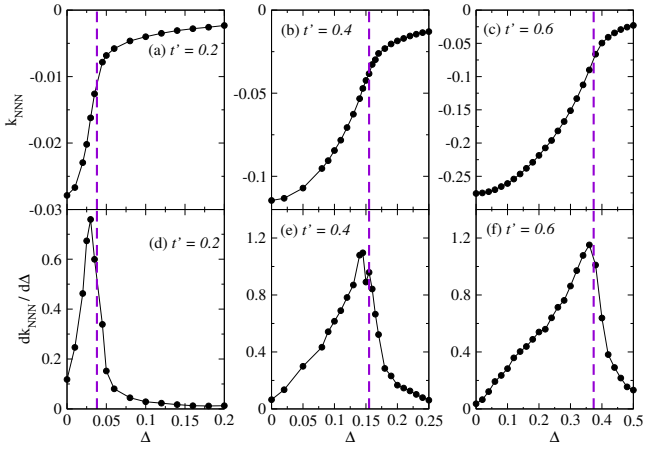

FIG. 6. (Color online) The kinetic energy associated with next-nearest neighbor hopping as a function of Δ for different values of t' in systems with $U = -4$ and 14×14 sites. The vertical dashed lines show the value of Δ_c as obtained in the finite-size scaling analysis of the pair structure factor.

14×14 lattice. A kink can be seen in the behavior of this observable around (slightly after) the critical value of Δ obtained in the finite size scaling of the pair structure factor (see the following subsection).

Another local quantity that exhibits a clear signature of the superconductor to Mott-insulator transition is the kinetic energy associated with next-nearest neighbor hoppings, i.e., $k_{NNN} = -(t'/N)\sum_{\langle\langle \boldsymbol{ij}\rangle\rangle,\sigma}\langle \hat{c}^\dagger_{\boldsymbol{i}\sigma}\hat{c}_{\boldsymbol{j}\sigma} + \hat{c}^\dagger_{\boldsymbol{j}\sigma}\hat{c}_{\boldsymbol{i}\sigma}\rangle)$, where $N = L \times L$. As shown in Figs. 6(a)–6(c), the absolute value of k_{NNN} decreases with increasing Δ. This observable also exhibits a kink right after Δ_c as predicted by the scaling analysis. The derivatives of k_{NNN} with respect to Δ, shown in Figs. 6(d)–6(f), exhibit clear peaks about Δ_c with maxima right before the value of Δ_c reported in the phase diagram.

Summarizing, the ED and the PDQMC results for various observables studied indicate the occurrence of the superconductor to Mott-insulator transition at approximately the same value of Δ as the fidelity metric. Hence, the results reported in the phase diagram (Fig. 1) are robust against the selection of the observable.

Universality class of the transition

The PDQMC calculations have the advantage that they allow us to study much larger lattice sizes and, after a proper finite-size scaling analysis, determine Δ_c in the thermodynamic limit. We take the pair structure factor $P = \sum_{i,j}\langle \hat{P}_j \hat{P}_i^\dagger\rangle$, with $\hat{P}_i = \hat{c}_{\boldsymbol{i}\uparrow}\hat{c}_{\boldsymbol{i}\downarrow}$, to be the order parameter to locate the superconductor to Mott-insulator transition (as mentioned in the previous section, other observables give similar results). The limit $|U|/t \gg 1$, for $t' = 0$, provides guidance on the nature of the superconductor to Mott-insulator transition for strong attractive interactions. Second-order perturbation theory in $t/|U|$ reveals that Eq. (1) becomes equivalent to a Hamiltonian for hard-core bosons with site creation (annihilation) operator $\hat{b}_i^\dagger = \hat{P}_i^\dagger$ ($\hat{b}_i = \hat{P}_i$) [24, 35] in a superlattice. The phase diagram for the latter model was studied in Refs. [36, 37] in two (2D) and three (3D) dimensions. At half-filling, this model exhibits a superfluid to Mott-insulator transition with increasing Δ that belongs to the $(d{+}1)$-XY universality class [36, 37], like the integer filling Mott transition in the Bose-Hubbard model [38]. The addition of t' to the hard-core boson model does not break its particle-hole symmetry. Hence, it does not qualitatively change the phase diagram in Refs. [36, 37].

Remarkably, at half-filling, the pair structure factor can be written as $P = \sum_{i,j}\langle \hat{P}_i^\dagger \hat{P}_j\rangle$, i.e., it maps onto the zero momentum mode occupation in the hard-core boson model, $m_{k=0} = \sum_{i,j}\langle \hat{b}_i^\dagger \hat{b}_j\rangle$. In the insulating phase of the latter quantum system in 2D one expects $\langle \hat{b}_i^\dagger \hat{b}_{i+r}\rangle \propto r^{-(1+\eta)}e^{-r/\xi}$ at long distances, as in the corresponding disordered 3D classical phase, where $\eta(= 0.0381 \pm 0.0002$ [39]) is the anomalous scaling dimension and ξ the correlation length. Near the transition, $m_{k=0}$ diverges with ξ as $m_{k=0} \sim \xi^{1-\eta}$ [40, 41] and the fraction f_0 of pairs that condense in a finite system ($\xi \to L$) vanishes as $f_0 \sim L^{-(1+\eta)}$ [40, 41]. Hence, f_0 scales as $f_0 L^{1+\eta} = F(|\Delta - \Delta_c|L^{1/\nu})$ [41], with $\nu = 0.6717 \pm 0.0001$ [39]. Turning back to fermions, we can write

$$(P/N_{\rm pairs})L^{1+\eta} = F(|\Delta - \Delta_c|L^{1/\nu}), \qquad (4)$$

where the number of pairs is $N_{\rm pairs} = L^2/2$.

Figure 7 shows the scaled pair-structure factor vs Δ for two values of U and two values of t'. In all cases the curves cross at a single point (Δ_c), as expected from the

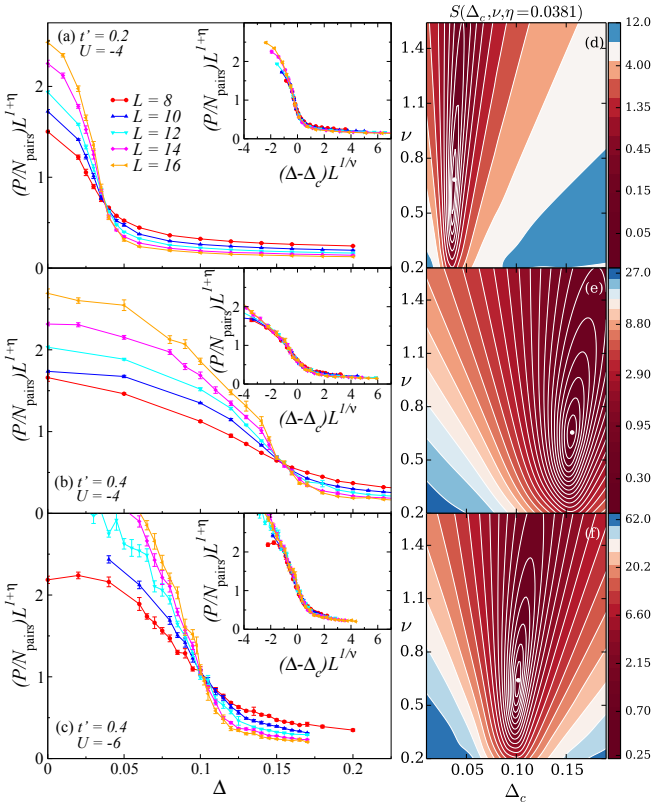

FIG. 7. (Color online) (a)–(c) show the scaled pair-structure factor as a function of Δ for different values of U and t'. The curves cross at Δ_c. The insets, show the scaling collapse for the same parameters as in the main panels. (d)–(f) show contour plots of the sum of the squared residuals $S(\Delta_c, \nu, \eta)$ of fits of F with eight-degree polynomials, for the parameters in panels (a)–(c), respectively. We set the value of η to 0.0381 [39] and found the minima of S, as signaled by the white dots, for the unknown parameters ν and Δ_c. ν at the minima is close to the expected $\nu = 0.67$ result.

scaling ansatz (4). That point moves toward larger values of Δ, from Fig. 7(a) to Fig. 7(b), as t' is increased at constant U, and moves toward smaller values of Δ, from Fig. 7(b) to Fig. 7(c), as $|U|$ is increased at constant t'. The insets show that, close to the crossing points, the data exhibits an almost perfect collapse according to the scaling ansatz (4). To further test this scaling hypothesis, we calculate the sum of the squared residuals $S(\Delta_c, \nu, \eta = 0.0381)$ of fits of F with high-order polynomials (orders 6, 8 and 10) in a fine mesh of values for Δ_c and ν. The value of ν at which S is minimum for those polynomials is close to $\nu = 0.67$, and the average value is 0.65 ± 0.08, 0.66 ± 0.04 and 0.64 ± 0.02 [42] for the parameters in Figs. 7(a)–7(c), respectively. These analyses show that, for those values of U, the superconductor to Mott-insulator transition in our *fermionic* model belongs to the 3D XY universality class. This despite the fact that the results are for a regime in which $|U|$ is of the order of 1/2 the bandwidth of the noninteracting system with $\Delta = t' = 0$ and, as such, strong coupling perturbation theory is not appropriate to describe the system. A compilation of crossing points as those in Fig. 7 allowed us to generate the phase diagram in Fig. 1(b). Unfortunately, for $|U| < 4$ and $t' \neq 0$, the values of the projection parameters Θ needed to obtain ground-state results are too large and the PDQMC calculations become prohibitively long and unstable, so we do not report results in the phase diagram for $|U| < 4$. Still, for $U = -4$, we can compare the ED and PDQMC results. They show that the values of Δ_c in the former are overestimated due to finite size effects.

Charge excitations

The observed universality class of the superconductor–Mott-insulator transition indicates that the lowest-energy charge excitations have bosonic character in *both* the superconducting and insulating phases near the transition. However, those excitations must be fermionic deep in the insulating phase. The insulating region with bosonic low-energy excitations is the s-wave equivalent of the pseudogap state (a crossover regime rather than a thermodynamic phase). In what follows, we explore when the lowest charge excitations change from bosonic to fermionic. In Fig. 8, we show the ground-state energy at half-filling as well as the energies of the lowest excited states with two extra fermions ($S^z = 0$, lowest energy bosonic excitation) and an extra fermion ($S^z = 1/2$, lowest energy fermionic excitation) as a function of Δ for two values of U and two values of t'.

Figures 8(a) and 8(b) show that, for the values of Δ at which the superconductor to Mott-insulator transition occurs for $U = -6$, the lowest energy excitations in both phases are bosonic. However, there is a value of $\Delta > \Delta_c$ for which those excitations (within the Mott phase) change from bosonic to fermionic. That value of Δ decreases as t' increases [Fig. 8(a) vs Fig. 8(b)] and as U decreases [left vs right panels in Fig. 8]. For $U = -4$ [Figs. 8(c) and 8(d)], the ED calculations predict that the transition from bosonic to fermionic excitations occurs in the Mott phase for $t' = 0$ and in the superconducting phase for $t' = 0.2$. The latter is attributed to finite size effects as it contradicts the expectation from the PDQMC results. Also, in the weak coupling limit, field-theory arguments anticipate the transition to be in the XY universality class [43, 44]. These results are nontrivial, even though any attractive short-range potential gives rise to bound states (Cooper "molecules") in 2D, because if interactions are not strong enough those "molecules" need not be small in comparison to the interparticle separation, i.e., bound-state condensation need not occur.

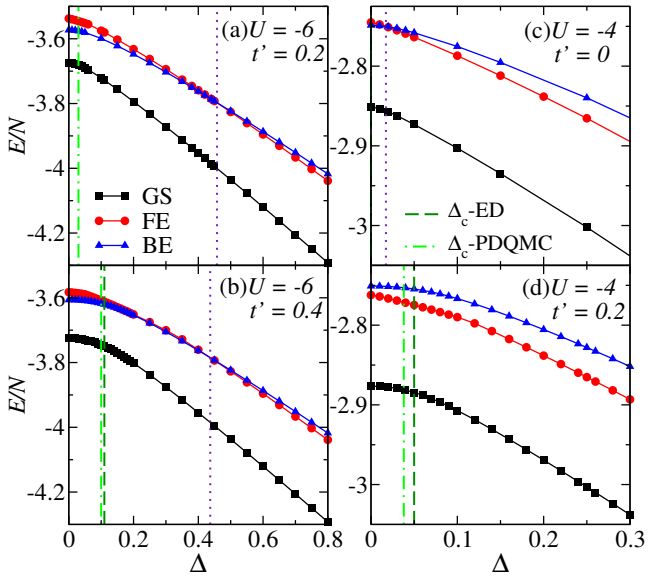

FIG. 8. (Color online) ED results for the ground state energy (GS), as well as the energies of the first fermionic (FE) and bosonic (BE) charge excitations vs Δ for different values of U and t'. The crossing points between the BE and FE curves (marked by the vertical dotted line) signal a change in the character of the lowest charge excitations. We report the energies per particle, E/N where N is the total number of particles, in 4×4 lattices. Dashed and dash-dotted line signal the superconductor-insulator transition using ED and PDQMC, respectively.

SUMMARY

We have introduced and studied a 2D model that undergoes a superconductor to insulator transition. We determined its phase diagram using ED and PDQMC calculations, and showed that, in the parameter regime accessible to PDQMC, the transition belongs to the $3D$-XY universality class. Our results echo the well-known XY transition of the bosonic Hubbard model, but in a *fermionic* system. We explored the nature of the lowest energy charge excitations and showed that they change from bosonic to fermionic in the insulating phase. Our numerical demonstration of "pseudogap" physics in a realizable model enables a new route for the experimental exploration of high-temperature superconductivity using ultracold atoms. While there are many microscopic differences between our model and real superconductors, there are also several universal similarities that can be exploited. Most notably, the dynamics of our system shares a lot in common with charge and vortex dynamics near the superconducting transition in layered or quasi-2D superconductors.

ACKNOWLEDGMENTS

This work was supported by the National Science Foundation Grants No. PHY13-18303 (R.M.,M.R.) and PHY-1205571 (P.N.), and by CNPq (R.M.). The computations were performed in the Institute for Cyber-Science at Penn State, the Center for High-Performance Computing at the University of Southern California, and CENAPAD-SP.

[1] J. Bardeen, L. N. Cooper, and J. R. Schrieffer, Physical Review **108**, 11751204 (1957).
[2] Y. Ando, G. S. Boebinger, A. Passner, T. Kimura, and K. Kishio, Physical Review Letters **75**, 4662 (1995).
[3] J. Corson, R. Mallozzi, J. Orenstein, J. N. Eckstein, and I. Bozovic, Nature **398**, 221 (1999).
[4] Y. Wang, Z. A. Xu, T. Kakeshita, S. Uchida, S. Ono, Y. Ando, and N. P. Ong, Physical Review B **64**, 224519 (2001).
[5] J. E. Hoffman, E. W. Hudson, K. M. Lang, V. Madhavan, H. Eisaki, S. Uchida, and J. C. Davis, Science **295**, 466 (2002).
[6] T. Valla, A. V. Fedorov, J. Lee, J. C. Davis, and G. D. Gu, Science **314**, 1914 (2006).
[7] K. K. Gomes, A. N. Pasupathy, A. Pushp, S. Ono, Y. Ando, and A. Yazdani, Nature **447**, 569572 (2007).
[8] Y. Kohsaka, C. Taylor, Wahl, A. Schmidt, J. Lee, K. Fujita, J. W. Alldredge, K. McElroy, J. Lee, H. Eisaki, Uchida, D.-H. Lee, and J. C. Davis, Nature **454**, 1072 (2008).
[9] G. Ghiringhelli, M. L. Tacon, M. Minola, S. Blanco-Canosa, C. Mazzoli, N. B. Brookes, G. M. D. Luca, A. Frano, D. G. Hawthorn, F. He, T. Loew, M. M. Sala, D. C. Peets, M. Salluzzo, E. Schierle, R. Sutarto, G. A. Sawatzky, E. Weschke, B. Keimer, and L. Braicovich, Science **337**, 821 (2012).
[10] T. Esslinger, Annual Review of Condensed Matter Physics **1**, 129 (2010).
[11] R. Jördens, N. Strohmaier, K. Günter, H. Moritz, and T. Esslinger, Nature (London) **455**, 204 (2008).
[12] U. Schneider, L. Hackermuller, S. Will, T. Best, I. Bloch, T. A. Costi, R. W. Helmes, D. Rasch, and A. Rosch, Science **322**, 1520 (2008).
[13] R. A. Hart, P. M. Duarte, T.-L. Yang, X. Liu, T. Paiva, E. Khatami, R. T. Scalettar, N. Trivedy, D. Huse, and R. G. Hulet., ArXiv:1407.5932.
[14] C. Chin, R. Grimm, P. Julienne, and E. Tiesinga, Rev. Mod. Phys. **82**, 1225 (2010).
[15] J. Sebby-Strabley, M. Anderlini, P. S. Jessen, and J. V. Porto, Phys. Rev. A **73**, 033605 (2006).
[16] S. Fölling, S. Trotzky, P. Cheinet, M. Feld, R. Saers, A. Widera, T. Müller, and I. Bloch, Nature **448**, 1029 (2007).
[17] P. J. Lee, M. Anderlini, B. L. Brown, J. Sebby-Strabley, W. D. Phillips, and J. V. Porto, Phys. Rev. Lett. **99**, 020402 (2007).
[18] H. Lignier, C. Sias, D. Ciampini, Y. Singh, A. Zenesini, O. Morsch, and E. Arimondo, Phys. Rev. Lett. **99**, 220403 (2007).

[19] A. Zenesini, H. Lignier, D. Ciampini, O. Morsch, and E. Arimondo, Phys. Rev. Lett. **102**, 100403 (2009).

[20] G. Jotzu, M. Messer, R. Desbuquois, M. Lebrat, T. Uehlinger, D. Greif, and T. Esslinger, Nature **515**, 237 (2014).

[21] L.-M. Duan, Physical review letters **95**, 243202 (2005).

[22] R. B. Diener and T.-L. Ho, Physical review letters **96**, 010402 (2006).

[23] J. K. Chin, D. Miller, Y. Liu, C. Stan, W. Setiawan, C. Sanner, K. Xu, and W. Ketterle, Nature **443**, 961 (2006).

[24] R. Micnas, J. Ranninger, and S. Robaszkiewicz, Rev. Mod. Phys. **62**, 113 (1990).

[25] A. Muramatsu, "Quantum monte carlo methods in physics and chemistry," (Kluwer Academic, 1999) pp. 343–373.

[26] F. F. Assaad, "Quantum simulations of complex many-body systems: From theory to algorithms," (John von Neumann Institute for Computing (NIC), 2002) pp. 99–155.

[27] P. Zanardi and N. Paunković, Phys. Rev. E **74**, 031123 (2006).

[28] L. CamposVenuti and P. Zanardi, Phys. Rev. Lett. **99**, 095701 (2007).

[29] P. Zanardi, P. Giorda, and M. Cozzini, Phys. Rev. Lett. **99**, 100603 (2007).

[30] M.-F. Yang, Phys. Rev. B **76**, 180403 (2007).

[31] M. Rigol, B. S. Shastry, and S. Haas, Phys. Rev. B **80**, 094529 (2009).

[32] C. N. Varney, K. Sun, V. Galitski, and M. Rigol, Phys. Rev. Lett. **107**, 077201 (2011).

[33] C. J. Jia, B. Moritz, C.-C. Chen, B. S. Shastry, and T. P. Devereaux, Phys. Rev. B **84**, 125113 (2011).

[34] R. Jördens, N. Strohmaier, K. Günter, H. Moritz, and T. Esslinger, Nature **455**, 204 (2008).

[35] S. Robaszkiewicz, R. Micnas, and K. A. Chao, Phys. Rev. B **23**, 1447 (1981).

[36] I. Hen and M. Rigol, Phys. Rev. B **80**, 134508 (2009).

[37] I. Hen, M. Iskin, and M. Rigol, Phys. Rev. B **81**, 064503 (2010).

[38] M. P. A. Fisher, P. B. Weichman, G. Grinstein, and D. S. Fisher, Phys. Rev. B **40**, 546 (1989).

[39] M. Campostrini, M. Hasenbusch, A. Pelissetto, and E. Vicari, Phys. Rev. B **74**, 144506 (2006).

[40] L. Pollet, N. V. Prokof'ev, and B. V. Svistunov, Phys. Rev. Lett. **104**, 245705 (2010).

[41] J. Carrasquilla and M. Rigol, Phys. Rev. A **86**, 043629 (2012).

[42] Error bars are defined as the 2σ standard deviation of the values of ν, which minimize the sum of square residuals for the three polynomials, from the mean.

[43] P. Nikolić and Z. Tešanović, Phys. Rev. B **83**, 064501 (2011).

[44] P. Nikolić, Phys. Rev. B **83**, 064523 (2011).